Epileptic Seizure Detection Based on Stockwell Transform and Bidirectional Long Short-Term Memory

Minxing Geng, Weidong Zhou, Guoyang Liu, Chaosong Li, and Yanli Zhang

***Abstract*— Automatic seizure detection plays a significant role in monitoring and diagnosis of epilepsy. This paper presents an efficient automatic seizure detection method based on Stockwell transform (S-transform) and bidirectional long short-term memory (BiLSTM) neural networks for intracranial EEG recordings. First, S-transform is applied to raw EEG segments, and the obtained matrix is grouped into time-frequency blocks as the inputs fed into BiLSTM for feature selecting and classification. Afterwards, post-processing is adopted to improve detection performance, which includes moving average filter, threshold judgment, multichannel fusion, and collar technique. A total of 689 h intracranial EEG recordings from 20 patients are used for evaluation of the proposed system. Segment-based assessment results show that our system achieves a sensitivity of 98.09% and specificity of 98.69%. For the event-based evaluation, a sensitivity of 96.3% and a false detection rate of 0.24/h are yielded. The satisfactory results indicate that this seizure detection approach possess promising potential for clinical practice.**

***Index Terms*— Automatic seizure detection, bidirectional long short-term memory, Stockwell transform.**

I. Introduction

EPILEPSY is a common neurological disease, which is characterized by abrupt, abnormal, and excessive electrical disturbances of brain neurons. According to the estimation of WHO, more than 50 million people worldwide suffer from medically intractable epilepsy [1]. Electroencephalography (EEG) has been widely applied to the diagnosis of brain diseases [2]–[4]. Long-term EEG recordings usually are visually analyzed by certified neurologists to identify abnormal seizure activities in clinical practice [3], which is a burdensome and tedious task. Therefore, the development of automatic seizure detection system is valuable for helping medical staff to relieve workload and monitor epilepsy.

Automatic seizure detection has been investigated for several decades and many encouraging results have been achieved. One of the earliest epileptic seizure detection systems was presented by Gotman [5] in the early 1980s. In his work, EEG signals were broken down into half waves, and slope, rhythmicity, and sharpness were extracted as features for classification. Later, this method was improved by Gotman [6] and Qu [7] to learn a patient specific false alarm model. After that, many approaches have been proposed, mainly including time domain [8]–[11], frequency domain [12]–[16], and nonlinear dynamics theory [17]–[24]. Yuan *et al.* [25] utilized pattern match regularity statistics to extract EEG features and employed extreme learning machine to address the imbalances between nonseizure and seizure data. Kumar *et al.* [26] computed the histograms of 1-D local binary pattern for the discriminant analysis. Acharya *et al.* [27] developed a 13-layer deep convolutional neural network (CNN) for categorizing seizure, pre-ictal and normal data. Siuly *et al.* [28] proposed to using Hermite transform for feature extraction and least square vector machine for classification. Supriya *et al.* [29] built a weight visibility graph network for seizure detection by measuring different strengths in graph theory. Ullah *et al.* [30] designed a pyramidal 1D-CNN model with two augmentation schemes for real-time seizure detection.

Due to the nonstationarity of EEG signals, many time-frequency techniques such as Short-time Fourier transform (STFT) and wavelet transform (WT) have been applied for EEG analysis. Stockwell transform (S-transform) proposed by Stockwell *et al.* [31] is considered as the combination of STFT and WT, which could realize multiresolution analysis with low computing complexity [32]. S-transform has been widely applied in many fields, such as heart sound segmentation [33], power quality analysis [34], and medical imaging [35]. In the current study, S-transform is utilized for time-frequency representation of EEG signals.

With the growth of mass data and the progress of parallel computing, deep learning has developed rapidly in many fields, such as computer vision [36], [37], natural language processing [38], [39] and the diagnosis of diseases [40].

Manuscript received June 19, 2019; revised October 9, 2019 and December 27, 2019; accepted January 7, 2020. Date of publication January 13, 2020; date of current version March 6, 2020. This work was supported in part by the Key Program of the Natural Science Foundation of Shandong Province under Grant ZR2013FZ002, in part by the Development Program of Science and Technology of Shandong under Grant 2014GSF118171, in part by the Research Funds of Science and Technology Innovation Committee of Shenzhen Municipality under Grant JCYJ20180305164357463, and in part by the Project of Shandong Province Higher Educational Science and Technology Program under Grant J17KA067. *(Corresponding author: Weidong Zhou.)*

Minxing Geng is with the School of Microelectronics, Shandong University, Jinan 250100, China (e-mail: gengminxing1995@163.com).

Weidong Zhou is with the School of Microelectronics, Shandong University, Jinan 250100, China, and also with the Shenzhen Research Institute of Shandong University, Shenzhen 518057, China (e-mail: wdzhou@sdu.edu.cn).

Guoyang Liu and Chaosong Li are with the School of Microelectronics, Shandong University, Jinan 250100, China (e-mail: virter1995@outlook.com; 201812113@mail.sdu.edu.cn).

Yanli Zhang is with the School of Information and Electronic Engineering, Shandong Technology and Business University, Yantai 264005, China (e-mail: sdlslily@163.com).

Digital Object Identifier 10.1109/TNSRE.2020.2966290

The recurrent neural network (RNN) is a kind of deep learning framework which exploits recurrent connections between network blocks. RNN possesses the ability to learn underlying dynamics of the sequential input [41] and has been extensively applied to analyze time series [42]. However, the main problem in the training of deep RNN is the gradient vanishing caused by overlong transmission during backpropagation. To address this limitation, long short-term memory (LSTM) with the inclusion of controlled gates is introduced by Hochreiter and Schmidhuber [43]. LSTM has an advantage over other neural networks in analyzing dynamic EEG signals, and has been used for emotion recognition [44], sleep stage classification [45] and seizure detection [46]–[48]. In the current work, bidirectional LSTM (BiLSTM) is applied to EEG time-frequency matrix obtained with S-transform. Compared with the feedforward LSTM, bidirectional LSTM (BiLSTM) could process time series in both time directions simultaneously [49], and has proven to have better capabilities in classification task [50].

This work presents an effective seizure detection algorithm which combines the S-transform and BiLSTM. S-transform has the advantages over Fourier transform and Wavelet transform in its low computational complexity. The time-frequency matrix obtained from S-transform is automatically feature selected and classified through BiLSTM. The public Freiburg EEG database is employed to evaluate the performance of our approach. To the best of our knowledge, this is the first attempt to combine S-transform and recurrent neural networks for seizure detection. Experimental results evidence the effectiveness of the proposed algorithm. Moreover, the combination of RNN with S-transform will also be beneficial to analyzing other biomedical data.

The rest of this paper is organized as follows. Section II gives a brief introduction of Freiburg intracranial EEG database. Section III is devoted to the proposed seizure detection method, which contains S-transform, BiLSTM, and postprocessing. The experimental results are exhibited in Section IV. Section V discusses the results and compare the performance with other algorithms. Section VI presents a conclusion of this paper.

II. Intracranial EEG Database

The intracranial EEG database used in this study comes from the Epilepsy Center of the University Hospital of Freiburg, Germany [51]. It contains invasive EEG recordings of 21 patients suffering from medically intractable epilepsy. The EEG was sampled by NT digital video EEG system and 16-bit A/D converter with the sampling rate of 256 Hz. Six EEG contacts which consist of three extra-focal and three in-focal channels were chosen by well-trained epileptologist. In our study, only the in-focal channels are utilized to train the model as they contain more physiological and pathological information.

For each patient, there are about 2-5 h seizure recordings in “Ictal” dataset and long term inter-ictal recordings in “Interictal” dataset, respectively. The former dataset contains seizure events which range from 12 seconds to 16 minutes and has at least 50 minutes of pre-ictal data. The latter dataset contains approximately 24 h of nonseizure EEG signals while patient 12 is an exception, who has about 48 h of interictal EEG data. All the beginning and the end of seizure events were notated by epileptologists according to the epileptic patterns and clinical manifestation.

TABLE I
Details of Used EEG Database

Patient	Seizure origin	Seizure type	Mean seizure durations(s)
1	temporal	CP,SP	13.1
2	frontal	GTC,CP,SP	118.2
3	temporal	CP,SP	105
4	temporal	GTC,CP,SP	87.4
5	frontal	GTC,CP,SP	44.9
6	temporal	GTC,CP	66.9
7	temporal	GTC,CP,SP	153.5
8	temporal	CP,SP	163.7
9	frontal	GTC,CP	114.7
11	frontal	GTC,CP,SP	157.3
12	frontal	GTC,CP,SP	55.1
13	temporal	GTC,CP,SP	158.3
14	temporal	GTC,CP	216.4
15	frontal	GTC,CP,SP	145.4
16	temporal	GTC,CP,SP	121.0
17	temporal	GTC,CP,SP	86.2
18	temporal	CP,SP	13.7
19	frontal	GTC,CP,SP	12.5
20	temporal	GTC,CP,SP	85.7
21	temporal	CP,SP	83.1
Total	-	-	100.1

Note: GTC = generalized tonic-clonic seizure, CP = complex partial seizures, SP = simple partial seizures,

To address the data imbalance between the seizure and nonseizure class, data augmentation technique is applied to the training set to minimize overfitting [52]. For each patient, we randomly select one or two seizure events and take the number of normal EEG recordings that are 5 times as seizure data in the training set. Then data augmentation is performed on the seizure data in the way that each seizure event is resampled five-fold. Finally, the amounts of nonseizure and seizure data are equal in the training set.

The details of used Freiburg database are presented in Table I. Note that patient 10 is not considered with the reason of electrode box disconnection. In summary, the training samples contain 0.82 h seizure recordings and 4.1 h normal recordings. About 680 h EEG recordings with 55 seizures from 20 patients are employed for the evaluation of the proposed method.

III. Method

The architecture of the proposed automatic seizure detection algorithm is depicted in Fig.1. The whole algorithm can be divided into three parts: Stockwell transform, bidirectional LSTM, postprocessing. Each part will be described particularly in the following sections.

A. Stockwell Transform

Due to the EEG’s nonstationarity, time-frequency analysis of EEG signals is helpful for detecting seizures [53]. Stockwell transform (S-transform) is an ideal time-frequency decomposition method, which combines the superiorities of short-time Fourier transform (STFT) and

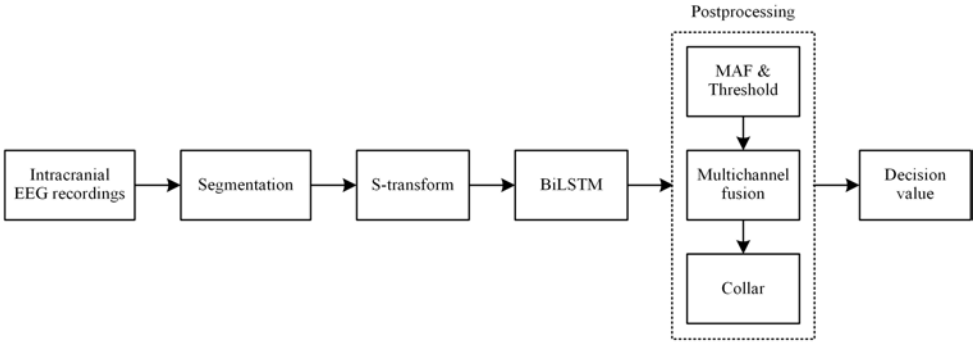

Fig. 1. Block diagram of proposed method for seizure detection.

wavelet transform (WT). The S-transform $S_x(\tau, f)$ of time domain signal $x(t)$ is defined by:

$$S_x(\tau, f) = e^{i2\pi f t} W_x(\tau, d) \tag{1}$$

$$W_x(\tau, d) = \int_{-\infty}^{+\infty} x(t) w(t-\tau, d) dt \tag{2}$$

where $W_x(\tau, d)$ denotes the wavelet transform of $x(t)$ and $w(t, f)$ is the Guassian window which is chosen as follows:

$$w(t, f) = \frac{|f|}{\sqrt{2\pi}} e^{\frac{-t^2 f^2}{2}} \tag{3}$$

Finally, the expression of S-transform is given as follows:

$$S_x(\tau, f) = \int_{-\infty}^{+\infty} x(t) \frac{|f|}{\sqrt{2\pi}} e^{\frac{-t^2 f^2}{2}} e^{-i2\pi f t} dt \tag{4}$$

The Gaussian window in (4), which is related to frequency f, could provide better frequency resolution at lower frequencies and better time resolution at higher frequencies. The S-transform spectrogram is given as:

$$S_{psd}(\tau, f) = S_x(\tau, f) S_x^*(\tau, f) \tag{5}$$

In the current work, EEG recordings are partitioned into 4 s segments (1024 points) with no overlapping. The S-transform of each segment returns a 1024 × 128 time-frequency matrix, where 128 corresponds to the frequency from 1 to 128 Hz, and 1024 stands for time points. Generally, the frequency range of seizure activity focuses on 3 to 30 Hz. Thus, the frequency range of the proposed S-transform spectrogram is chosen from 4 to 32 Hz. Besides, to decrease the computation complexity of our system, the time-frequency matrix is divided into 64 blocks in time axis and 14 blocks in frequency axis. 896 blocks are generated by accumulating the power in each block. At last, a 14 × 64 matrix is obtained after the S-transform in this study, which will be used as the input of BiLSTM.

Fig 2 and Fig 3 illustrate the difference between normal and seizure EEG segment randomly selected from patient 9. Fig 2(a) and Fig 3(a) depict normal and seizure EEG segments. In Fig 2(b) and Fig 3(b), the y-axis stands for the frequency ranging from 4 to 32 Hz, and the depth of color indicates the power at corresponding time-frequency block.

B. Bidirectional Long Short-Term Memory

The recurrent neural network (RNN) is proven to be an efficient deep network for solving time-series problems. It has been successfully implemented in natural language process and speech recognition. Through a feedback connection in RNN, previous information in sequential data can be utilized by the following state [39]. The main problem existing in the training process of RNN is gradient vanishing or exploding. To address those problems, the RNN unit is replaced with a gated memory cell called long short term memory (LSTM). With the special controlling gate and memory blocks, LSTM helps to maintain gradients during back-propagation and allows the network to remember long term information. Fig.4 depicts the structure of single LSTM cell which includes five components: the memory cell c_t, the candidate memory c'_t, forget gate f_t, input gate i_t, and output gate o_t.

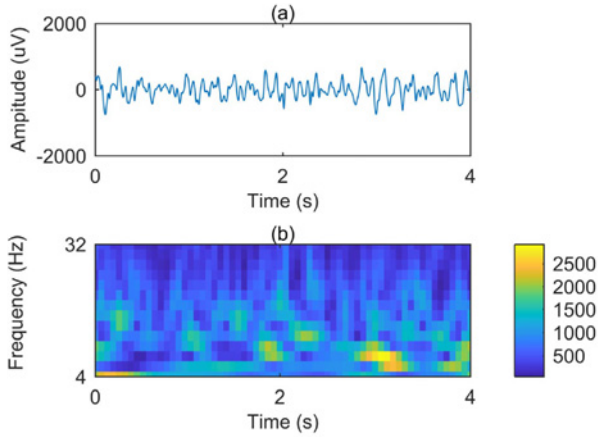

Fig. 2. (a) normal EEG signal (b) S-transform of normal EEG.

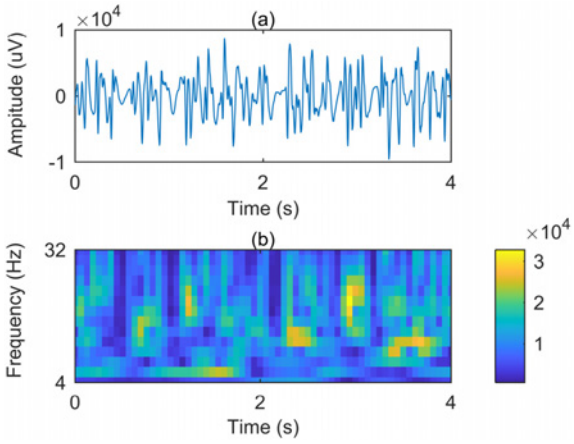

Fig. 3. (a) seizure EEG signal (b) S-transform of seizure EEG.

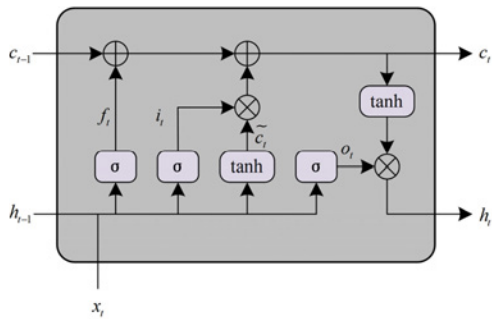

Fig. 4. Structure of a LSTM cell.

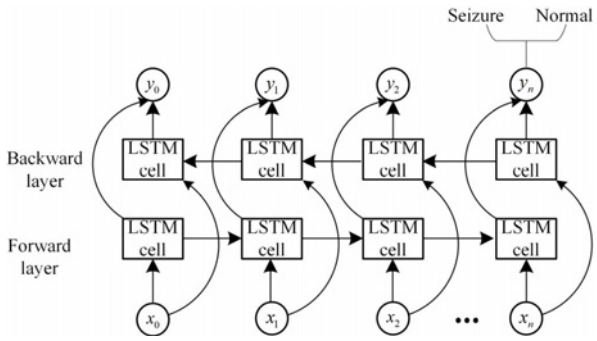

Fig. 5. Architecture of proposed BiLSTM.

Consider a time sequence input $X = (x_1, x_2, x_3, \ldots x_n)$. At time t, given input x_t, and the hidden state h_{t-1} from previous time, the procedure of LSTM network can be divided as follows:

$$f_t = \sigma(W_{fh} \cdot h_{t-1} + W_{fx} \cdot x_t + b_f) \quad (6)$$
$$i_t = \sigma(W_{ih} \cdot h_{t-1} + W_{ix} \cdot x_t + b_i) \quad (7)$$
$$o_t = \sigma(W_{oh} \cdot h_{t-1} + W_{ox} \cdot x_t + b_o) \quad (8)$$
$$c'_t = \tanh(W_{ch} \cdot h_{t-1} + W_{cx} \cdot x_t + b_c) \quad (9)$$
$$c_t = f_t \cdot c_{t-1} + i_t \cdot c'_t \quad (10)$$
$$h_t = o_t \cdot \tanh(c_t) \quad (11)$$

where $\sigma(\cdot)$ is the sigmoid function, W represents weight matrices, b denotes biases.

Whether the information to be remembered or forgotten is decided by forget gate f_t in (6). Input gate i_t calculates the degree to which the new content is added to the next memory cell by using (7). o_t in (8) is the output gate which determines the part of the memory content that will be exposed. The candidate cell is calculated in (9). The new cell c_t in (10) is obtained by adding the previous information through the forget gate and the new information through the input gate. The LSTM output at time t can be computed by using (11).

In feedforward LSTMs, information flows from forward to backward. BiLSTM is proposed to exploit information flowing in two directions. The structure of BiLSTM used in this study is depicted in Fig.5. The last output of BiLSTM is followed with a fully connected layer which uses softmax as activation function to map the inputs into probability values. The sum of all probabilities is equal to 1. The expression of softmax function can be defined as:

$$y_j^{(i)} = \frac{e^{z_j^{(i)}}}{\sum_{j=1}^{C} e^{z_j^{(i)}}} \quad (12)$$

For each patient, we trained three models for the three focal channels respectively. Differential operating is performed to the softmax layer, and output score of single channel ranges from -1 to 1.

The whole neural network avoids overfitting by using adaptive moment estimation (Adam) as optimizer and L2 regularization. The hyper parameters used in this neural network are listed as follows: learning rate = 0.001, batch size = 20, LSTM hidden units = 40, L2 regularization rate = 0.0001, and training_epochs = 100.

C. Postprocessing

For improving detection performance, postprocessing is performed to the output scores of BiLSTM, which contains smoothing, threshold decision, multichannel fusion and collar operation [54].

To remove random noise and sharp spikes, a moving average filter is carried out to the output score, which can be defined as:

$$z(i) = \frac{1}{2M+1} \sum_{k=-M}^{M} x(i+k) \quad (13)$$

where z is the filtered signal, x denotes the output of BiLSTM,, $2M + 1$ represents the length of smoothing. In this study, the smoothing length is between 5 to 15, which is specific for different patients. The smoothing process is beneficial to exclude some accidental burrs.

Then the filtered signal is compared with a fixed threshold *Thr* to obtain a binary label. *Thr* is specific for each patient which is calculated during training procedure. If the value after smoothing is bigger than *Thr*, the segment will be labeled as 1, otherwise as 0. The threshold operation achieves binary decisions, where 1 denotes seizure segment and 0 represents nonseizure segment.

Multichannel fusion is employed in the next step to improve detection accuracy and reduce misjudgment. In the three focal channels, if a testing segment is detected as seizure at least in two channels, it will be marked as a seizure segment; if the segment is detected as seizure in single channel but its adjacent segment is detected, it will also be labeled as a seizure segment. Otherwise, it will be declared as a normal segment.

The start and the end of seizure events become more obscurely due to the smoothing procedure. Hence, a collar operation is deployed to compensate for these missed parts [55]. In this study, each seizure activity detected by our approach is extended at either side to prevent the misjudgment of seizure. The example of postprocessing procedure selected from patient 17 is illustrated in Fig.6.

IV. Results

All experiments were carried out in Matlab R2018a and Tensorflow 1.11.0 environment (Python 3.6) running on a core processor unit with 3.60 GHz. Two evaluation criteria have been employed for the performance evaluation of the proposed seizure detection algorithm: the segment-based criterion and the event-based criterion.

For the segment-based level, three statistical measurements are introduced by comparing the labels marked by our method

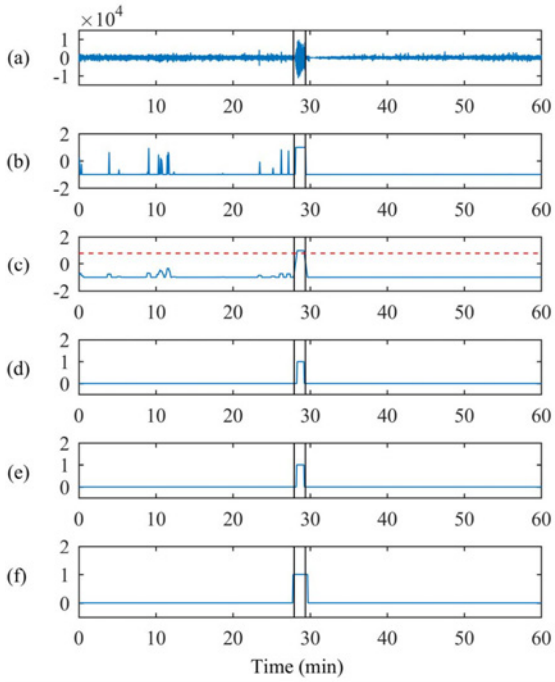

Fig. 6. The postprocessing procedure of 1h EEG data. (a) 1h origin EEG recording in channel 1. (b) Decision outputs of BiLSTM classifier in channel 1. (c) The data in channel 1 after smoothing. (d) The binary value after threshold in channel 1. (e) The multi-channel fusion results after the three channel integration. (f) The final decisions after collar technique. The seizure event marked by experts is between the two vertical lines.

with those judged by neurologists, which can be expressed as:

$$Sensitivity = \frac{TP}{TP + FN} \times 100\% \quad (14)$$

$$Specificity = \frac{TN}{TN + FP} \times 100\% \quad (15)$$

$$Accuracy = \frac{TP + TN}{TP + FN + TN + FP} \times 100\% \quad (16)$$

Here, TP (true positive) denotes the segments labeled as seizure by both our method and experienced neurologists. TN (True Negative) represents the segments marked as normal by our method and neurologists. FP (False Positive) denotes the number of detected seizure segment identified by our system but marked as real normal segment by experts. FN (False Negative) represents the number of seizure segments incorrectly labeled by the detection algorithm.

The results of segment-based metrics are presented in Table II. On average, the sensitivity of 98.09%,the specificity of 98.69% and the accuracy of 98.69% are obtained. Moreover, there are 15 patients having the sensitivity of 100%, while 18 patients' specificities have exceeded 99%. Due to the missed detection, the sensitivities of patient 14, 19 are relatively low, which are 87.10% and 83.33% respectively.

For the event-based level, two measures are applied to assess the performance of the proposed approach in clinical practice: event based sensitivity and false detection rate. The event-based sensitivity is calculated through the number of true detections dividing by the number of testing seizures for each patient. False detection rate (FDR) represents the mean times of false positive events in an hour.

TABLE II
DETECTION RESULTS OF PROPOSED METHOD ON EPOCH-BASED METRICS

Patient	Sensitivity (%)	Specificity (%)	Accuracy (%)
1	100	98.95	98.95
2	100	99.21	99.22
3	100	99.88	99.88
4	100	99.18	99.18
5	100	92.30	92.30
6	100	98.65	98.65
7	100	98.27	98.28
8	100	98.30	98.30
9	97.96	98.09	98.09
11	100	99.79	99.79
12	100	99.45	99.45
13	100	97.42	97.43
14	87.10	99.48	99.43
15	93.46	98.65	98.75
16	100	98.75	98.75
17	100	99.68	99.68
18	100	98.76	98.76
19	83.33	99.77	99.77
20	100	99.46	99.46
21	100	99.72	99.72
Total	98.09	98.69	98.69

TABLE III
DETECTION RESULTS OF PROPOSED METHOD ON EVENT-BASED METRICS

Patient	Number of experts-marked seizures	Number of true detections	Sensitivity(%)	FDR (/h)
1	2	2	100	0.516
2	2	2	100	0.25
3	3	3	100	0
4	3	3	100	0.09
5	4	4	100	1.01
6	2	2	100	0.13
7	2	2	100	0.53
8	1	1	100	0.25
9	4	4	100	0.375
11	2	2	100	0
12	3	3	100	0.156
13	1	1	100	0.25
14	3	2	66.7	0.03
15	3	3	100	0.21
16	4	4	100	0.37
17	4	4	100	0
18	3	3	100	0.51
19	2	1	50	0.06
20	4	4	100	0
21	3	3	100	0.08
Total	55	53	96.3	0.24

Note: FDR = false detection rate

The results of event-based evaluation are summarized in Table III. For event-based evaluation, the mean sensitivity of 96.3% and mean FDR of 0.24/h are achieved. Furthermore, all patients except patient 14 and 19 have no undetected seizures. The highest false detection rate occurs at patient 15 owing to the artifacts which contains spikes and resemble seizure activities.

V. DISCUSSION

A seizure detection algorithm combining S-transform and BiLSTM is presented in current work. S-transform is performed to intracranial EEG recordings and the time- frequency

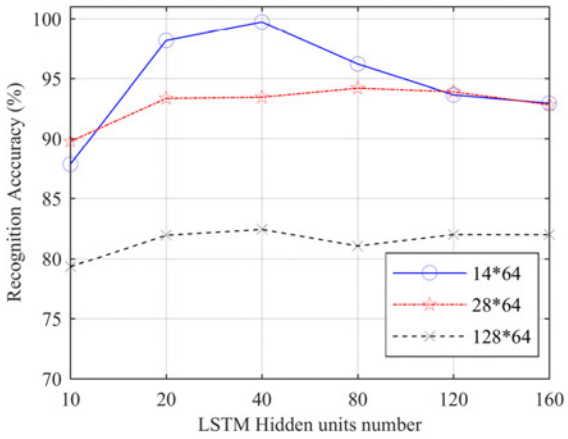

Fig. 7. Comparison of epoch-based accuracies under different S-transform features and LSTM hidden units.

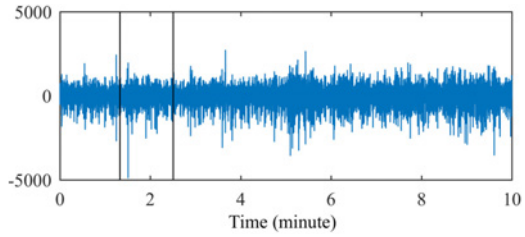

Fig. 8. A missing seizure detection of patient 14. The seizure event marked by experts is between the two vertical lines.

matrix is obtained. A bidirectional LSTM network is served as a feature selector and classifier, and postprocessing is used to improve the accuracy of classification.

Compared with other time-frequency approaches, S-transform has proven to be efficient in investigating the dynamic EEG signals due to its multiresolution analysis capability and low time complexity. In this study, the output of S-transform on a 4-s EEG epoch is a 128 × 1024 matrix. To reduce the complexity of BiLSTM network, we select the frequency band from 4 to 32 Hz, and divide the time axis into 64 blocks, which significantly reduces the time for training BiLSTM. The number of parameters in BiLSTM is given as follows:

$$n_{parameters} = 2 \times \left(4 \times \left(n_{input} \times n_{output} + 1\right) \times n_{input}\right) \quad (17)$$

The input size of LSTM is chosen as 14, which correspond to the frequency axis of S-transform matrix. And the output size denotes the hidden units in each single LSTM block. Too many parameters in neural networks may cause the problem of overfitting, whereas few parameters will limit the fitting ability of the model. Here we use patient 20 to compare the influences of different parameters, and the comparison is shown in Fig.7. It is noted that the performance of 14 × 64 S-transform matrix with 40 hidden units in LSTM block achieves 99.72% recognition accuracy in patient 20.

Figure 8 depicts a missing seizure detection from patient 14. The seizure is not obvious compared with the background activity, which may be the reason of this missing detection.

Table IV summaries the results of four cases, including LSTM, BiLSTM, LSTM with S-transform, and BiLSTM with S-transform. For LSTM and BiLSTM without S-transform,

TABLE IV
PERFORMANCE COMPARISON

Method	Sensitivity (%)	Specificity (%)	FDR(/h)
LSTM	77.74	84.37	0.91
BiLSTM	82.86	89.21	1.10
LSTM with S-transform	93.29	98.93	0.47
BiLSTM with S-transform	98.08	98.69	0.24

TABLE V
DETECTION RESULTS WITHOUT POSTPROCESSING

Patient	Sensitivity (%)	Specificity (%)	Accuracy (%)
1	78.21	98.99	98.98
2	100	99.27	99.27
3	96.7	99.91	99.91
4	94.08	99.23	99.23
5	93.75	93.45	93.45
6	88.5	98.77	98.77
7	100	98.31	98.31
8	100	99.02	99.02
9	96.32	98.54	98.55
11	100	99.79	99.79
12	100	99.65	99.64
13	93.5	97.75	97.75
14	75.4	99.62	99.62
15	81.5	98.92	98.92
16	100	99.01	99.01
17	88.45	99.72	99.72
18	65	99.11	99.11
19	77.5	99.79	99.79
20	98	99.61	99.61
21	97.15	99.84	99.84
Total	91.2	98.91	98.91

the overall sensitivity and specificity are 77.84%, 84.37% and 82.86%, 89.21%, respectively, and for LSTM and BiLSTM combined with S-transform, the sensitivity and specificity are 93.29%, 98.93% and 98.98%, 98.69%, respectively, which indicates the effectiveness of S-transform for EEG time-frequency representation. Furthermore, in the comparison of LSTM and BiLSTM with S-transform, the average improvement in sensitivity is 4.79%, which demonstrates that the BiLSTM possesses better capabilities for feature selection and classification.

In this work, postprocessing is used to improve detection performance. Table V presents the detection results without postprocessing, and the mean sensitivity and specificity are 91.2 % and 98.97% respectively. Compared with Table II, it could be noted that the procedure of postprocessing results in a notable increase in sensitivity which improves from 91.2% to 98.09%. Meanwhile, there is only a slight decline in specificity.

To quantify the time cost of our system, we calculated the running time in the training and testing stage on a Dell workstation with a 3.6GHz Intel processor running Matlab R2018a and Tensorflow 1.11.0. For each patient, the average time taken in training stage and testing stage are about 48 s and 3 s respectively. On the Freiburg EEG database, Li *et al.* [56] proposed an improved sparse representation method for seizure

TABLE VI
COMPARISON OF PERFORMANCES FOR DIFFERENT METHODS PROPOSED IN RECENT YEARS

Method	Epoch-based sensitivity (%)	Total of data (h)	False detection rate (/h)	Number of patients used	Year
S-transform and singular value decomposition [58]	96.40	183.07	0.16	20	2015
Dictionary pair learning [59]	93.39	530	0.236	20	2018
Cross-bispectrum analysis[60]	95.83	560	0.24	20	2019
DWT with random forests[61]	99.74	28.6	0.21	21	2019
Kernel robust probabilistic collaborative representation [62]	97.48	564.38	0.57	21	2019
Our proposed method	98.09	689.1	0.24	20	-

detection, which took about 11 s for the training stage and 50 s for 1h EEG testing data. Yuan *et al.* [57] presented a kernel collaborative representation method, which consumed about 15s in training stage and 1min for 1h EEG recordings in testing stage. In comparison with their methods, the time complexity in training stage is relatively longer due to the training of deep neural network, but the time consumed in testing stage in our algorithm is 3 s for one hour recordings, which can meet the need of real-time seizure detection.

The Freiburg Epilepsy EEG database has been applied in several previous studies for evaluation. The comparison results between our method and other seizure detection methods are listed in Table VI. Xia *et al.* [58] developed a seizure detection system based on S-transform and singular value decomposition (SVD). The algorithm was tested on 183 h EEG signals from 20 patients and yielded overall sensitivity of 96.40% as well as a false detection rate of 0.16/h. Even though they have obtained a lower FDR compared with our method, the sensitivity in our algorithm is higher and the testing set is much bigger than theirs. In the work of Ma and Yu [59], a novel dictionary pair learning algorithm was built for seizure detection. Three channels of EEG from 20 patients with 55 seizures were used for experiment, and they gained a lower epoch-based sensitivity of 93.39% with a false detection rate of 0.236/h.

Recently, Mahmoodian *et al.* [60] used cross bispectrum as features and obtained a sensitivity of 95.83%. Tzimourta *et al* [61] integrated DWT features with random forest classifier. They tested their method on 28.6 h data and attained a high sensitivity of 99.74%. Yu *et al.* [62] proposed a collaborative representation method using kernel robust probabilistic and achieved 97.48% sensitivity on 21 patients. Compared to those works, our proposed approach shows competitive performance and yields a sensitivity of 98.09% with the longest length of EEG data.

VI. CONCLUSION

In this work, an efficient approach based on S-transform and BiLSTM has been proposed for automatic seizure detection. EEG segments are time-frequency represented by using S-transform, and BiLSTM are employed as feature extractor and classifier. The approach is evaluated on the Freiburg Epilepsy database and yields a sensitivity of 98.09% and a specificity of 98.69% on the epoch-based level. Besides, a sensitivity of 96.36% and 0.24/h false detection rate are achieved under event-based level. The prominent performance suggests that this method has the potential of clinical application.

REFERENCES

[1] *Epilepsy*, World Health Org., Geneva, Switzerland, 2019. [Online]. Available: https://www.who.int/en/news-room/fact-sheets/detail/epilepsy
[2] H. Adeli, Z. Zhou, and N. Dadmehr, "Analysis of EEG records in an epileptic patient using wavelet transform," *J. Neurosci. Methods*, vol. 123, no. 1, pp. 69–87, Feb. 2003.
[3] S. J. M. Smith, "EEG in the diagnosis, classification, and management of patients with epilepsy," *J. Neurol., Neurosurgery Psychiatry*, vol. 76, no. 2, pp. 2–7, Jun. 2005.
[4] S. Siuly, L. Yan, and Z. Yanchun, *EEG Signal Analysis and Classification: Techniques and Applications*. Heidelberg, Germany: Springer, 2016.
[5] J. Gotman, "Automatic recognition of epileptic seizures in the EEG," *Electroencephalogr. Clin. Neurophysiol.*, vol. 54, no. 5, pp. 530–540, Nov. 1982.
[6] J. Gotman, "Automatic seizure detection: Improvements and evaluation," *Electroencephalogr. Clin. Neurophysiol.*, vol. 76, no. 4, pp. 317–324, Oct. 1990.
[7] H. Qu and J. Gotman, "Improvement in seizure detection performance by automatic adaptation to the EEG of each patient," *Electroencephalogr. Clin. Neurophysiol.*, vol. 86, no. 2, pp. 79–87, Feb. 1993.
[8] A. T. Tzallas, M. G. Tsipouras, and D. I. Fotiadis, "Epileptic seizure detection in EEGs using time–frequency analysis," *IEEE Trans. Inf. Technol. Biomed.*, vol. 13, no. 5, pp. 703–710, Sep. 2009.
[9] L. Logesparan, A. J. Casson, and E. Rodriguez-Villegas, "Optimal features for online seizure detection," *Med. Biol. Eng. Comput.*, vol. 50, no. 7, pp. 659–669, Jul. 2012.
[10] K. Samiee, P. Kovacs, and M. Gabbouj, "Epileptic seizure classification of EEG time-series using rational discrete short-time Fourier transform," *IEEE Trans. Biomed. Eng.*, vol. 62, no. 2, pp. 541–552, Feb. 2015.
[11] E. Kabir, J. Cao, and H. Wang, "A computer aided analysis scheme for detecting epileptic seizure from EEG data," *Int. J. Comput. Intell. Syst.*, vol. 11, no. 1, pp. 663–671, Apr. 2018.
[12] P. Rana, J. Lipor, H. Lee, W. Van Drongelen, M. H. Kohrman, and B. Van Veen, "Seizure detection using the phase-slope index and multichannel ECoG," *IEEE Trans. Biomed. Eng.*, vol. 59, no. 4, pp. 1125–1134, Apr. 2012.
[13] H. Khamis, A. Mohamed, and S. Simpson, "Frequency-moment signatures: A method for automated seizure detection from scalp EEG," *Clin. Neurophysiol.*, vol. 124, no. 12, pp. 2317–2327, Dec. 2013.
[14] F. Riaz, A. Hassan, S. Rehman, I. K. Niazi, and K. Dremstrup, "EMD-based temporal and spectral features for the classification of EEG signals using supervised learning," *IEEE Trans. Neural Syst. Rehabil. Eng.*, vol. 24, no. 1, pp. 28–35, Jan. 2016.

[15] H. R. Al Ghayab, Y. Li, S. Siuly, and S. Abdulla, "Epileptic EEG signal classification using optimum allocation based power spectral density estimation," *IET Signal Process.*, vol. 12, no. 6, pp. 738–747, Aug. 2018.

[16] H. R. Al Ghayab, Y. Li, S. Siuly, and S. Abdulla, "Epileptic seizures detection in EEGs blending frequency domain with information gain technique," *Soft Comput.*, vol. 23, no. 1, pp. 227–239, Jan. 2019.

[17] E. D. Übeyli, "Lyapunov exponents/probabilistic neural networks for analysis of EEG signals," *Expert Syst. Appl.*, vol. 37, no. 2, pp. 985–992, Mar. 2010.

[18] A. Aarabi, R. Fazel-Rezai, and Y. Aghakhani, "A fuzzy rule-based system for epileptic seizure detection in intracranial EEG," *Clin. Neurophysiol.*, vol. 120, no. 9, pp. 1648–1657, Sep. 2009.

[19] H. Ocak, "Automatic detection of epileptic seizures in EEG using discrete wavelet transform and approximate entropy," *Expert Syst. Appl.*, vol. 36, no. 2, pp. 2027–2036, Mar. 2009.

[20] N. Kannathal, M. L. Choo, U. R. Acharya, and P. Sadasivan, "Entropies for detection of epilepsy in EEG," *Comput. Methods Programs Biomed.*, vol. 80, no. 3, pp. 187–194, Dec. 2005.

[21] R. Zarei, J. He, S. Siuly, G. Huang, and Y. Zhang, "Exploring Douglas-Peucker algorithm in the detection of epileptic seizure from multicategory EEG signals," *BioMed Res. Int.*, vol. 2019, pp. 1–19, Jul. 2019.

[22] S. Taran, V. Bajaj, and S. Siuly, "An optimum allocation sampling based feature extraction scheme for distinguishing seizure and seizure-free EEG signals," *Health Inf. Sci. Syst.*, vol. 5, no. 1, 2017, Art. no. 7.

[23] H. R. Al Ghayab, Y. Li, S. Siuly, and S. Abdulla, "A feature extraction technique based on tunable Q-factor wavelet transform for brain signal classification," *J. Neurosci. Methods*, vol. 312, pp. 43–52, Jan. 2019.

[24] A. R. Hassan, S. Siuly, and Y. Zhang, "Epileptic seizure detection in EEG signals using tunable-Q factor wavelet transform and bootstrap aggregating," *Comput. Methods Programs Biomed.*, vol. 137, pp. 247–259, Dec. 2016.

[25] Q. Yuan *et al.*, "Epileptic seizure detection based on imbalanced classification and wavelet packet transform," *Seizure*, vol. 50, pp. 99–108, Aug. 2017.

[26] T. S. Kumar, V. Kanhangad, and R. B. Pachori, "Classification of seizure and seizure-free EEG signals using local binary patterns," *Biomed. Signal Process. Control*, vol. 15, pp. 33–40, Jan. 2015.

[27] U. R. Acharya, S. L. Oh, Y. Hagiwara, J. H. Tan, and H. Adeli, "Deep convolutional neural network for the automated detection and diagnosis of seizure using EEG signals," *Comput. Biol. Med.*, vol. 100, pp. 270–278, Sep. 2018.

[28] S. Siuly, O. F. Alcin, V. Bajaj, and A. Sengur, "Exploring hermite transformation in brain signal analysis for the detection of epileptic seizure exploring hermite transformation in brain signal analysis for the detection of epileptic seizure," *IET Sci. Meas. Technol.*, vol. 13, no. 1, pp. 35–41, 2018.

[29] S. Supriya, S. Siuly, H. Wang, J. Cao, and Y. Zhang, "Weighted visibility graph with complex network features in the detection of epilepsy," *IEEE Access*, vol. 4, pp. 6554–6566, 2016.

[30] I. Ullah, M. Hussain, E.-U.-H. Qazi, and H. Aboalsamh, "An automated system for epilepsy detection using EEG brain signals based on deep learning approach," *Expert Syst. Appl.*, vol. 107, pp. 61–71, Oct. 2018.

[31] R. Stockwell, L. Mansinha, and R. Lowe, "Localization of the complex spectrum: The S transform," *IEEE Trans. Signal Process.*, vol. 44, no. 4, pp. 998–1001, Apr. 1996.

[32] M. Kıymık, İ. Güler, A. Dizibüyük, and M. Akın, "Comparison of STFT and wavelet transform methods in determining epileptic seizure activity in EEG signals for real-time application," *Comput. Biol. Med.*, vol. 35, no. 7, pp. 603–616, Oct. 2005.

[33] A. Moukadem, A. Dieterlen, N. Hueber, and C. Brandt, "A robust heart sounds segmentation module based on S-transform," *Biomed. Signal Process. Control*, vol. 8, no. 3, pp. 273–281, May 2013.

[34] P. K. Dash, B. K. Panigrahi, and G. Panda, "Power quality analysis using S-transform," *IEEE Trans. Power Del.*, vol. 18, no. 2, pp. 406–411, Apr. 2003.

[35] S. Assous, A. Humeau, M. Tartas, P. Abraham, and J. L'huillier, "S-transform applied to laser Doppler flowmetry reactive hyperemia signals," *IEEE Trans. Biomed. Eng.*, vol. 53, no. 6, pp. 1032–1037, Jun. 2006.

[36] C. Szegedy *et al.*, "Going deeper with convolutions," in *Proc. IEEE Conf. Comput. Vis. Pattern Recognit. (CVPR)*, Jun. 2015, pp. 1–9.

[37] Y. LeCun, Y. Bengio, and G. Hinton, "Deep learning," *Nature*, vol. 521, no. 7553, pp. 436–444, 2015.

[38] G. E. Hinton *et al.*, "Deep neural networks for acoustic modeling in speech recognition," *IEEE Signal Process. Mag.*, vol. 29, no. 6, pp. 82–97, Oct. 2012.

[39] J. Schmidhuber, "Deep learning in neural networks: An overview," *Neural Netw.*, vol. 61, pp. 85–117, Jan. 2015.

[40] H.-C. Shin *et al.*, "Deep convolutional neural networks for computer-aided detection: CNN architectures, dataset characteristics and transfer learning," *IEEE Trans. Med. Imag.*, vol. 35, no. 5, pp. 1285–1298, May 2016.

[41] A. Petrosian, D. Prokhorov, R. Homan, R. Dasheiff, and D. Wunsch, "Recurrent neural network based prediction of epileptic seizures in intra- and extracranial EEG," *Neurocomputing*, vol. 30, nos. 1–4, pp. 201–218, Jan. 2000.

[42] P. Wang, A. Jiang, X. Liu, J. Shang, and L. Zhang, "LSTM-based EEG classification in motor imagery tasks," *IEEE Trans. Neural Syst. Rehabil. Eng.*, vol. 26, no. 11, pp. 2086–2095, Nov. 2018.

[43] S. Hochreiter and J. Schmidhuber, "Long short-term memory," *Neural Comput.*, vol. 9, no. 8, pp. 1735–1780, 1997.

[44] S. Alhagry, A. A. Fahmy, and R. A. El-Khoribi, "Emotion recognition based on EEG using LSTM recurrent neural network," *Int. J. Adv. Comput. Sci. Appl.*, vol. 8, no. 10, pp. 355–358, 2017.

[45] N. Michielli, U. R. Acharya, and F. Molinari, "Cascaded LSTM recurrent neural network for automated sleep stage classification using single-channel EEG signals," *Comput. Biol. Med.*, vol. 106, pp. 71–81, Mar. 2019.

[46] S. L. Oh, E. Y. Ng, R. S. Tan, and U. R. Acharya, "Automated diagnosis of arrhythmia using combination of CNN and LSTM techniques with variable length heart beats," *Comput. Biol. Med.*, vol. 102, pp. 278–287, Nov. 2018.

[47] K. M. Tsiouris, V. C. Pezoulas, M. Zervakis, S. Konitsiotis, D. D. Koutsouris, and D. I. Fotiadis, "A long short-term memory deep learning network for the prediction of epileptic seizures using EEG signals," *Comput. Biol. Med.*, vol. 99, pp. 24–37, Aug. 2018.

[48] R. Hussein, H. Palangi, R. K. Ward, and Z. J. Wang, "Optimized deep neural network architecture for robust detection of epileptic seizures using EEG signals," *Clin. Neurophysiol.*, vol. 130, no. 1, pp. 25–37, Jan. 2019.

[49] M. Schuster and K. Paliwal, "Bidirectional recurrent neural networks," *IEEE Trans. Signal Process.*, vol. 45, no. 11, pp. 2673–2681, Nov. 1997.

[50] A. Graves, N. Jaitly, and A.-R. Mohamed, "Hybrid speech recognition with deep bidirectional LSTM," in *Proc. IEEE Workshop Autom. Speech Recognit. Understand.*, Dec. 2013, pp. 273–278.

[51] G. Freiburg. (2008). *Freiburg Seizure Prediction Project*. [Online]. Available: http://epilepsy.uni-freburg.de/freiburg-seizure-prediction-project/eeg-database

[52] J. Salamon and J. P. Bello, "Deep convolutional neural networks and data augmentation for environmental sound classification," *IEEE Signal Process. Lett.*, vol. 24, no. 3, pp. 279–283, Mar. 2017.

[53] A. Yan *et al.*, "Automatic seizure detection using Stockwell transform and boosting algorithm for long-term EEG," *Epilepsy Behav.*, vol. 45, pp. 8–14, Apr. 2015.

[54] Y. Liu, W. Zhou, Q. Yuan, and S. Chen, "Automatic seizure detection using wavelet transform and SVM in long-term intracranial EEG," *IEEE Trans. Neural Syst. Rehabil. Eng.*, vol. 20, no. 6, pp. 749–755, Nov. 2012.

[55] A. Temko, E. Thomas, W. Marnane, G. Lightbody, and G. Boylan, "EEG-based neonatal seizure detection with Support Vector Machines," *Clin. Neurophysiol.*, vol. 122, no. 3, pp. 464–473, Mar. 2011.

[56] J. Li, W. Zhou, S. Yuan, Y. Zhang, C. Li, and Q. Wu, "An improved sparse representation over learned dictionary method for seizure detection," *Int. J. Neur. Syst.*, vol. 26, no. 1, Feb. 2016, Art. no. 1550035.

[57] S. Yuan *et al.*, "Kernel collaborative representation-based automatic seizure detection in intracranial EEG," *Int. J. Neur. Syst.*, vol. 25, no. 2, Mar. 2015, Art. no. 1550003.

[58] Y. Xia, W. Zhou, C. Li, Q. Yuan, and S. Geng, "Seizure detection approach using S-transform and singular value decomposition," *Epilepsy Behav.*, vol. 52, pp. 187–193, Nov. 2015.

[59] X. Ma, N. Yu, and W. Zhou, "Using dictionary pair learning for seizure detection," *Int. J. Neur. Syst.*, vol. 29, no. 4, May 2019, Art. no. 1850005.

[60] N. Mahmoodian, A. Boese, M. Friebe, and J. Haddadnia, "Epileptic seizure detection using cross-bispectrum of electroencephalogram signal," *Seizure*, vol. 66, pp. 4–11, Mar. 2019.

[61] K. D. Tzimourta *et al.*, "A robust methodology for classification of epileptic seizures in EEG signals," *Health Technol.*, vol. 9, no. 2, pp. 135–142, Mar. 2019.

[62] Z. Yu *et al.*, "Automatic seizure detection based on kernel robust probabilistic collaborative representation," *Med. Biol. Eng. Comput.*, vol. 57, no. 1, pp. 205–219, Jan. 2019.